TerraSAR-X 強度画像を用いた 2015 年ネパール地震における建物被害の抽出

Damage extraction of buildings in Kathmandu due to the 2015 Nepal Earthquake using TerraSAR-X intensity imagery

16TM0312　Rendy Bahri

指導教員　山崎　文雄
劉　ウェン

SYNOPSIS

Damage assessment is an important issue in emergency response and recovery after the occurrence of nature disasters. In this regard, remote sensing is recognized as an effective tool for detecting and monitoring affected areas. In this study, we used multi-temporal high-resolution TerraSAR-X images to detect the changes of urban areas in Kathmandu, the capital city of Nepal, which was severely affected by the 2015 Nepal Earthquake. It caused the collapse of many buildings including those in Kathmandu Durbar Square. TerraSAR-X images obtained before and after the earthquake were utilized for calculating the difference and correlation coefficient of the SAR backscatter, within the layover area of a large building in order to extract severely damaged buildings in the central Kathmandu. The affected areas were identified by high values of the difference and low values of the correlation coefficient. As the result, both of index was found to be the good suitable index to identify severely affected buildings.

1. Introduction

The 2015 Gorkha earthquake with Mw 7.8 occurred at 11:56 NST on 25 April in the central part of Nepal. A major aftershock with Mw 6.7 followed on 26 April 2015 in the same region at 12:55 NST. Due to the earthquake, centuries-old buildings were destroyed at UNESCO World Heritage sites in the Kathmandu Valley, including some at the Kathmandu Durbar Square. In order to grasp damage situation quickly after a natural disaster strikes, remote sensing is recognized as an effective tool. Especially, Synthetic Aperture Radar (SAR) sensors can observe objects on the earth surface without depending on the sunlight condition and under cloud-cover. Recently, the texture analysis of remotely sensed imagery becomes popular especially in land-cover classification.

In this study, TerraSAR-X images obtained before and after the earthquake as an emergency-response support are used to detect the affected areas in the Kathmandu area. The difference and correlation coefficient of each building was calculated in order to do extraction damage building.

2. The study area and imagery data used

Kathmandu, the capital and largest municipality of Nepal, was selected as the study area of this paper as shown in **Fig. 1**. Especially we focused on the central Kathmandu including the Durbar Square, one of the World heritage sites in Nepal.

Fig. 1 The Study area of the 2015 Nepal earthquake

In this study we used the images obtained by TerraSAR-X that was launched on 2007 by the German Aerospace Center (DLR). A pre-event SAR image was acquired on October 13, 2013 and a post-event image was acquired on April 27, 2015 (2 days after the earthquake). The acquisition mode of the images was Spotlight with VV polarization and an incidences angle of 39.5 degrees. **Fig. 2** shows a color composite of the pre- and post-event images, in which several changed areas could be confirmed by red (increased backscatter) and cyan (decreased backscatter) colors. The green square shows the target area, an enlarge images of this area shown in **Fig. 3(a)** Radiometric calibration for each intensity image was carried out to get the backscattering coefficient (sigma naught, σ^0). After this conversion, two pre-processing steps were applied. First, an adaptive filter[1] was applied to the original SAR images to reduce the speckle noise.

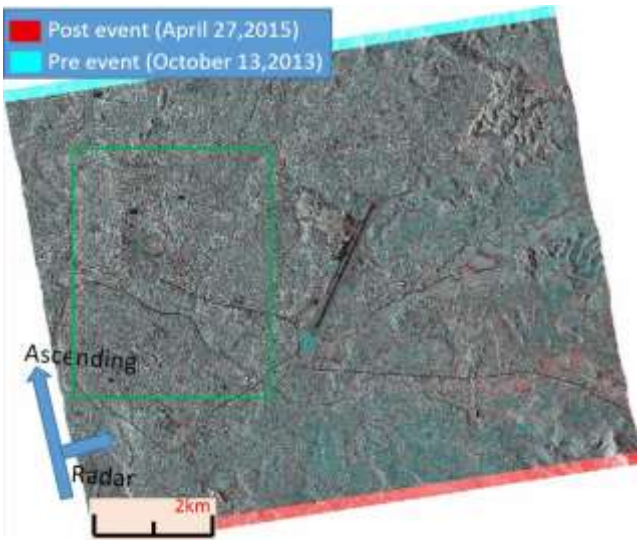

Fig. 2 Color composite of TerraSAR-X images in Kathmandu and the target area (Green square)

Pre-event and post-event high-resolution optical satellite images were also introduced as the truth data of building damage in the study area. The pre-event WorldView-3 (WV3) image was acquired on October 14, 2014 (04:59:37 UTC) with off-nadir angle 21° shown in **Fig. 3(b).**, and the post-event GeoEye-1 (GE1) image on May 15, 2015 (04:59:26 UTC) with off-nadir angle 23° shown in **Fig. 3(c).** For the two temporal images, the bundle products of the panchromatic (Pan) and four multi-spectral (BGR and near-IR) bands were introduced. After a pan sharpening process, the pre-event WV3 image has the spatial resolution of 31 cm and the post-event GE1 image 50 cm..

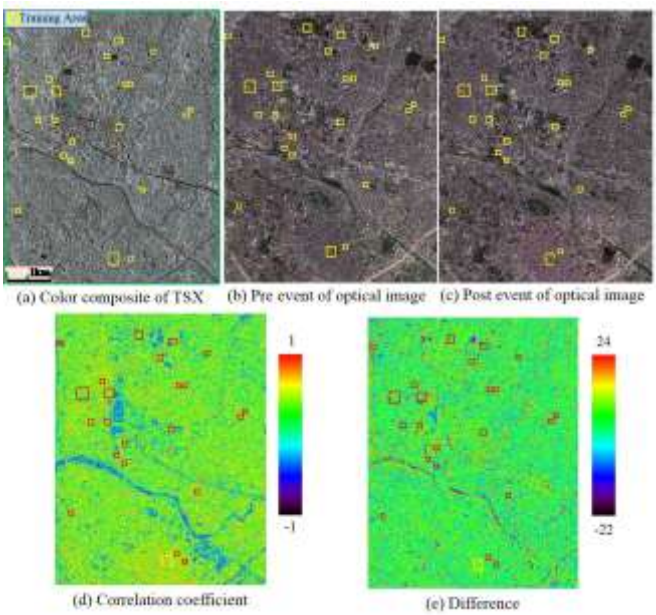

Fig. 3 Close-up of the central Kathmandu: (a) Color composite of the TSX images with the post-event (red) and pre-event (blue + green: cyan) ones; (b) Correlation coefficient; (c) Difference; (d) the pre-event WV-3 image on October 14, 2014; (e) the post-event GE-1 image on May 15, 2015.

3. Method of damage detection

The change detection from two-temporal SAR intensity images can be evaluated quantitatively by their backscattering difference value (d) and the correlation coefficient (r), calculated from **Equations (1) and (2)**. Due to the building size in the target area is around 10m - 15m, 11 × 11 pixels window (13.75m × 13.75m) was adopted to obtain d and r in this study.

$$r = \frac{N\sum_{i=1}^{N} Ia_i Ib_i - \sum_{i=1}^{N} Ia_i \sum_{i=1}^{N} Ib_i}{\sqrt{(N\sum_{i=1}^{N} Ia_i^2 - (\sum_{i=1}^{N} Ia_i)^2)\cdot (N\sum_{i=1}^{N} Ib_i^2 - (\sum_{i=1}^{N} Ib_i)^2)}} \quad (1)$$

$$d = \bar{I}a_i - \bar{I}b_i \quad (2)$$

$$L = \frac{H}{\tan\theta} \quad (3)$$

where Ia_i,Ib_i represent the i-th pixel vales of the post- and pre-event SAR backscattering coefficient values, respectively, and $\bar{I}a\_i$ and $\bar{I}b\_i$ are the average values of the 11×11 pixels surrounding the i-th pixel. The correlation coefficient (r) is a scalar quantity between -1.0 and 1.0, and used to find the measure of correspondence between two-sample populations. High positive value of r indicates no change between the pre- and post-event images whereas a low value indicates the strong possibility of change [2].

Fig. 3(d) shows the correlation coefficient of the backscattering coefficients (r) of the target area, ranging from -1.0 to 1.0 and **Fig. 3(e)** show the difference of backscattering coefficient (d), ranging from -22 dB to 24 dB, between the pre- and the post- event images.

In this study, we selected 22 training areas including 41 collapsed/major damaged buildings (G4-G5 in the EMS-98 scale, abbreviated as "collapsed") and 50 no/minor damage buildings (G1-G3 in the EMS-98 scale, abbreviated as "survived") in the target area, to explain the tendency of the relationship between damaged and non-damaged areas in the backscattering difference and the correlation coefficient. These training areas are shown in **Fig. 4**. The collapsed buildings are shown by red polygons and the survived buildings by green polygons. We selected them using the pre- and post-event optical images, field survey photos and aerial videos by drone. The break line shows the edge of the rooftop of a building, whereas the solid line shows the layover of a building's wall due to the oblique incidence of radar. The length of layover was calculated by **Equation (3)**, in which H is a building height and θ is the SAR incidence angle.

Fig.4. Training area in the central Kathmandu: 4 1Collapsed・Major damaged buildings and 50 No・Minor damaged buildings with rooftop and layover of each building

4. Detection Result

We calculated the average of correlation coefficient and the absolute difference of backscattering coefficients of the TSX images within the estimated layover area for each building, as shown in **Table 1**. The average of absolute difference for survived buildings was 0.67 dB with the standard deviation 0.52 dB, whereas the one for the collapsed buildings was 2.37 dB with standard deviation 1.78 dB. The collapsed buildings show high differences due to the change in the backscattering intensity. On the other hand, the average of correlation coefficient for 50 survived buildings was 0.42 with standard deviation 0.14. The high correlation value means the change before and after the earthquake was not significant. While the average of correlation coefficient for 41 collapsed buildings was 0.12 with standard deviation 0.19, which is quite low.

We can see the correlation coefficients for buildings Nos. 2, 4, 10, 16 are quite low compared with those of other survived buildings. As shown in **Fig. 4**, these low values were caused by the rubbles of collapsed buildings and the change of vegetation. On the other hand, the correlation coefficients for buildings Nos. 127, 131, 137, 143, 146, 147, 148, and 150 are quite high, which are supposed to be low due to the changes caused by the earthquake.

Table 1. Correlation coefficient and absolute difference of backscattering coefficient inside layover of the building.

No Major damage building			Bldg. No.	d [dB]	r
Bldg. No.	d [dB]	r	26	0.20	0.43
1	0.59	0.32	27	0.70	0.46
2	0.88	0.21	28	0.29	0.43
3	0.14	0.35	29	1.02	0.22
4	0.40	0.20	30	0.98	0.48
5	0.60	0.47	31	1.20	0.43
6	0.76	0.33	32	1.05	0.58
7	0.23	0.49	33	1.24	0.28
8	0.31	0.52	34	0.00	0.37
9	1.18	0.33	35	0.21	0.48
10	0.79	0.22	36	0.33	0.38
11	0.41	0.52	37	1.04	0.44
12	0.80	0.53	38	1.47	0.41
13	0.99	0.26	39	0.67	0.37
14	0.50	0.34	40	0.28	0.06
15	1.87	0.41	41	0.54	0.49
16	0.48	0.19	42	1.61	0.49
17	0.88	0.49	43	0.13	0.72
18	0.85	0.27	44	0.00	0.08
19	0.00	0.34	45	1.33	0.46
20	0.40	0.39	46	0.10	0.45
21	0.57	0.50	47	0.14	0.57
22	0.20	0.28	48	0.10	0.44
23	0.60	0.41	49	0.11	0.04
24	0.00	0.31	50	1.00	0.27
25	0.40	0.43	Average	0.67	0.42
			Std Deviation	0.52	0.14

Collapsed Major damage building			Bldg. No.	d [dB]	r
Bldg. No.	d [dB]	r	111	1.02	0.12
110	1.02	0.12	112	0.47	-0.21
111	0.47	-0.21	113	0.00	-0.27
112	0.00	-0.27	114	8.84	0.19
113	8.84	0.19	115	4.10	0.15
114	4.10	0.15	116	1.58	0.16
115	1.58	0.16	117	0.82	-0.11
116	0.82	-0.11	118	0.20	-0.10
117	0.20	-0.10	119	7.90	-0.02
118	2.31	0.26	120	0.61	0.20
119	7.90	-0.02	121	1.10	0.21
120	0.61	0.20	122	1.22	0.40
121	1.10	0.21	123	0.84	0.18
122	1.22	0.40	124	1.14	0.34
123	0.84	0.18	125	8.96	0.14
124	1.14	0.34	126	1.00	0.00
125	8.96	0.14	127	0.32	0.42
126	1.00	0.00	128	2.11	0.05
127	0.32	0.42	129	2.20	0.19
128	2.11	0.05	130	0.75	0.03
129	2.20	0.19	Average	2.37	0.12
130	0.75	0.03	Std Deviation	1.78	0.19

Bldg. No.	d [dB]	r
131	0.37	0.41
132	1.58	-0.03
133	0.27	0.10
134	1.89	-0.08
135	1.89	0.32
136	1.84	0.15
137	1.46	0.62
138	0.46	0.25
139	1.41	0.33
140	0.71	0.23
141	3.40	0.24
142	2.58	0.15
143	1.37	0.42
144	0.82	0.24
145	1.78	0.26
146	0.83	0.42
147	0.30	0.64
148	1.70	0.48
149	2.62	-0.01
150	2.13	0.45
Average	2.37	0.12
Std Deviation	1.78	0.19

The scatter diagram of the correlation coefficient and difference for collapsed and survived buildings is showed in **Fig. 5**. The collapsed buildings are shown by red triangles whereas the survived buildings by green circles. The average value for the collapsed buildings is shown by a black filled triangle, and that for the survived buildings by a black filled circle. The plus and minus standard deviations are shown by the error bar. From the figure, the correlation coefficient of the survived buildings is very high while the difference is close to zero, which indicates the change due the earthquake was small. On the other hand, the correlation coefficients of the collapsed buildings are low compared with those of the survived buildings, and their difference values are distributed widely.

In this study, we used these two indices to extract damaged buildings. In order to obtain the best threshold values for damage extraction, the cumulative distribution of the average values of the correlation coefficient within the layover area and that of the average value of the difference within the layover area are shown in **Fig. 6 (a)** and **(b)**, respectively. In these plots, the cumulative probability of the plotting point i is i/(n+1) with n indicating the number of samples.

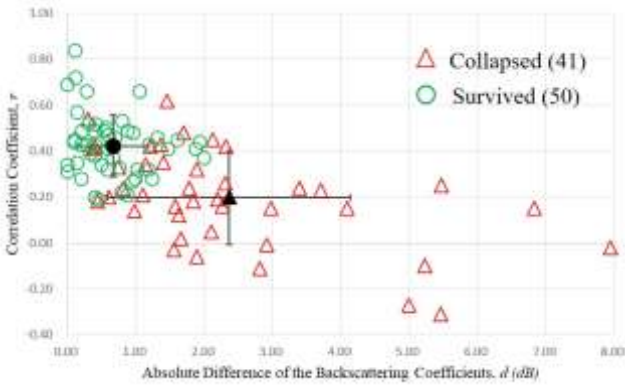

Fig. 5. Scatter diagram of correlation coefficient and difference of backscattering coefficient of the collapsed building and survived building

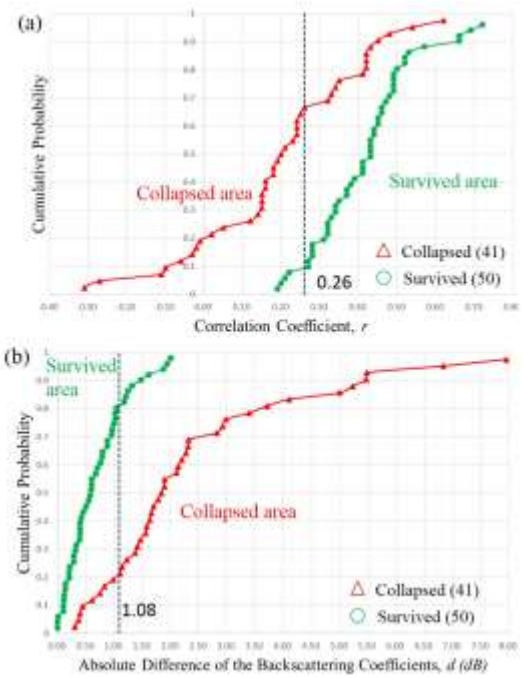

Fig. 6. Cumulative probability of the **(a)** correlation coefficient and **(b)** difference value of the 41 collapsed buildings and 50 survived building

Fig. 7(a) shows the change of the producer accuracy for collapsed buildings (red line), survived buildings (green line), and the sum of the both producer accuracies (yellow line), when the threshold of the correlation coefficient moves from -0.4 to 1.0 continuously. From this figure, the largest sum of the producer accuracies was obtained for the threshold value of 0.26 for the correlation coefficient. **Fig. 7(b)** shows the similar plot when the difference threshold moves from 0 dB to 8 dB. When the threshold of the difference was 1.33, the total producer accuracy became largest (165%) as shown in **Fig. 7(b)**. However, the goal of this study is to extract the collapsed buildings, so we chose 1.08 as the threshold of the difference that is possible to extract more collapsed buildings, compared with the threshold value 1.33. Then the total producer accuracy for the threshold 1.08 was 164.2%, 0.8% lower compared to the result for the threshold 1.33. We plot this threshold in **Fig. 6**. The left part of the threshold called “Collapsed area” whereas the right part of

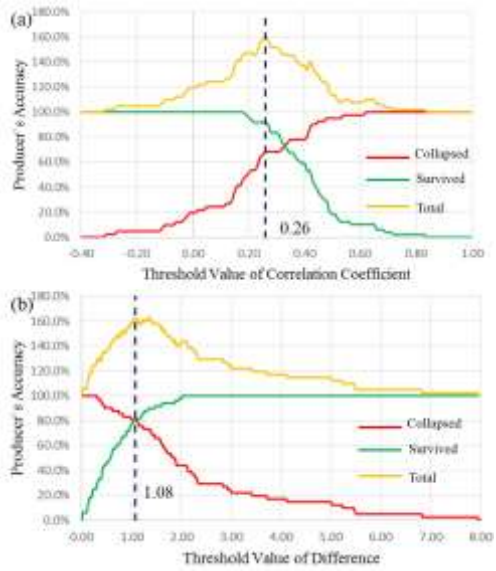

Fig. 6(a). When the threshold of correlation coefficient that moved from -0.4 to 1.0 continuously, the change of producer accuracy of collapsed (red line) and survived (green line) building and the total of the both producer accuracy (Yellow line); **(b)** show for the difference that moved from 0 dB to 8 dB.

the threshold called "Survived area". On the other hand, **Fig. 6(b)** shows the opposite of **Fig. 6(a)**. Four survived buildings entered "Collapsed area" while 13 collapsed buildings were misclassified as shown in **Fig. 6(a)**. **Fig. 6(b)** shows 8 collapsed buildings entered "Survived area" while 9 of 50 survived buildings were misclassified.

5. Accuracy Assessment: Confusion Matrix

The error matrix of the result based on the threshold values for the correlation coefficient and backscattering difference is shown in **Table 2.** According to this table, the producer's accuracy of the collapsed buildings is only 68.3% that is quite low compared to that for the survived buildings, which is 92.0%. On the other hand, the user's accuracy for collapsed buildings is quite high as 87.5% compared to the one for survived buildings, which is 78.0%. Thus, the overall accuracy based on the correlation coefficient is 81.3%. In this study, we selected 41 collapsed buildings and 50 survived buildings, which were the close population with high credibility. Many of previous studies used few collapsed buildings compared to survived buildings that made the overall accuracy quite high [3, 4]. In order to remove the random coincidence rate, we calculated the kappa coefficient for the correlation coefficient, which is 0.615. This value means substantial agreement for the correlation coefficient in this study. **Table 2** show the producer's accuracy of the collapsed building is 80.5%, which is almost the same with the one for survived buildings (82.0%). While the user's accuracy of collapsed building is 78.6% that is lower than the one for survived buildings (83.7%). Thus, the overall accuracy based on the difference threshold is 81.3%, the same to the result for the correlation coefficient. However, the kappa coefficient for the difference is 0.624, a bit higher than the result for the correlation coefficient.

Table 2. Error matrix classification of the result based on threshold of correlation coefficient and difference of backscattering coefficient.

		Correlation coefficient				Difference			
		Reference Data				Reference Data			
		Collapsed	Survived	Total	UA	Collapsed	Survived	Total	UA
Image Interpretation	Collapsed	28	4	32	87.5%	33	9	42	78.6%
	Survived	13	46	59	78.0%	8	41	49	83.7%
	Total	41	50	91		41	50	91	
	PA	68.3%	92.0%			80.5%	82.0%		
	Overall Accuracy				81.3%	Overall Accuracy			81.3%
	Kappa Coefficient				0.615	Kappa Coefficient			0.624

6. Conclusions

Recently satellite SAR data became one of the useful tools for detecting and monitoring affected areas due to natural disasters because SAR can capture the earth surface's condition both at daytime and night-time and under cloud-cover situation. In this study, multi-temporal high-resolution TerraSAR-X images were used for damage inspection of the Kathmandu area, which was severely affected by the Mw 7.8 Gorkha, Nepal earthquake on 25 April 2015. The SAR images obtained before and after the earthquake were utilized for calculating the difference and correlation coefficient of the backscattering coefficient values within the layover and roof-print of an individual building. We chose 41 collapsed buildings and 50 survived buildings in the central part of Kathmandu using the pre- and post-event high resolution optical images, aerial video footages, and field survey photos as references. The affected areas were characterized by a low correlation coefficient and a high absolute difference. A threshold value of the correlation coefficient and difference was determined for training areas in the central Kathmandu. As a result, the overall accuracy of correlation coefficient was 81.3% with the kappa coefficient 0.613, whereas the overall accuracy for the difference was also 81.3 % with the kappa coefficient 0.624, which indicates high level of agreement.

ACKNOWLEDGEMENT

The TerraSAR-X data are the property of the German Aerospace Center (DLR) and Inforterra GmbH and were made available by the PASCO Corporation through the joint research between PASCO Co. and Chiba University.

REFERENCES

1) Lee, J.S., Digital image enhancement and noise filtering by use of local statistics, IEEE Transaction on Pattern Analysis and Machine Intelligence, 2(2), 165-168, 1980.
2) Brown, L.G.: A survey of image registration techniques. ACM Computing Surveys, 24 (4), 1992.
3) Iwasaki, Y., Yamazaki, F., Liu, W., Nonaka, T., Sasagawa, T.: Detection of damage to building side-walls using high-resolution satellite SAR images. Journal of Japan Association for Earthquake Engineering, Vol. 13, No. 5, pp 18-32, 2013
4) Uprety, P., and Yamazaki, F., Dell' Acqua, F.. Damage detection using high-resolution SAR imagery in the 2009 L'Aquila, Italy, Earthquake. Earthquake Spectra, Vol. 29, No. 4, pp.1521-153, 2013